

Proton-induced spallation reactions between 300 MeV and 20 GeV

A. J. Cole and R. Cherkaoui-Tadili*

Institut des Sciences Nucléaires, 38026 Grenoble Cedex, France

(Received 2 February 1987)

Proton-induced spallation reactions are studied in the energy region from 300 MeV to 20 GeV. An analytical expression is derived for the production cross sections of target residues in which the incident proton energy dependence of the cross sections is described by variation of a single parameter. Rather good agreement is obtained with experiment when reasonable physical assumptions for the variation of this parameter are made.

I. INTRODUCTION

The present work was inspired by a paper of Abul-Magd, Friedman, and Hüfner¹ (and by an older paper by Campi and Hüfner²) in which the production of residues from targets of Au, Ag, and Cu was pictured as arising from what may be described as a low energy mechanism. Specifically, the incident proton is supposed to deposit a fraction of its kinetic energy in the target (via nucleon-nucleon collisions), which subsequently decays by successive emission of nucleons or heavier particles. Because the average mass loss from the target is roughly proportional to the average energy deposited, which, in turn, is proportional to the average number of nucleon-nucleon collisions, $T = \langle n \rangle$, it is clear that this latter quantity, which is essentially geometrical in nature, is a fundamental ingredient in the calculation of cross sections.

No attempt has been made in this work to improve on the physics contained in Ref. 1, which represents a greatly simplified image of what must surely be a rather complex process. On the contrary, we use results of Ref. 1 to concentrate the physics of the reaction mechanism into a single parameter which is the average mass emitted from the target per nucleon-nucleon collision. We do, however, show that a careful treatment of the reaction geometry allows us to obtain a rather good description of experimental excitation functions (or residue mass distributions) for protons incident on a Au target.

We divide this paper into five sections. Target nucleus geometry is described in Sec. II, the underlying (and greatly simplified) physics is the subject of Sec. III, Sec. IV compares calculations with experimental results, and, finally, Sec. V presents a summary and discussion.

II. GEOMETRY

A. Projection of nuclear densities

The fundamental quantity which determines the energy deposited by the incident proton in the target is assumed to be the average number of nucleon-nucleon collisions taking place between an incident proton at impact parameter b (fm) and the nucleons of the target nucleus¹⁻³ which, in the optical limit of Glauber theory,⁴ is given by

$$T(b) = \bar{\sigma}_{NN} \rho_p(b) = \bar{\sigma}_{NN} \int_{-\infty}^{\infty} \rho(r) dz, \quad (1)$$

where $\rho(r)$ is the target nuclear matter density and $\bar{\sigma}_{NN}$ is the free isospin averaged nucleon-nucleon cross section. Integrals over impact parameter (used to obtain cross sections) are, in general, not analytic if $\rho(r)$ has a Woods-Saxon (Fermi) form. In Ref. 5 for the case of intermediate energy nucleus-nucleus collisions an analytic form for dT/db^2 was proposed which enabled integrals over impact parameter (b) to be transformed into integrals over the average number of nucleon-nucleon collisions (T). It happens to be the case that this form is also suitable to describe the projected densities of atomic nuclei. We take

$$\frac{d\rho_p}{db^2} = -\rho_p e^{-k_p \rho_p} / 2\sigma^2, \quad (2)$$

which yields

$$b^2 / 2\sigma^2 = \text{Ei}[k_p \rho_p(0)] - \text{Ei}[k_p \rho_p(b)], \quad (3)$$

where $\text{Ei}(x)$ is the exponential integral. In Fig. 1 we show that Eq. (3) provides a good approximation to projected nuclear densities obtained by numerically integrating Woods-Saxon forms along the z coordinate. The three parameters (see Table I) σ , $\rho_p(0)$, and k_p were obtained for each nucleus as follows.

The numerically calculated projected densities are quite close to Gaussian forms for large impact parameter (this fact has been used by Karol⁶ to derive a simple analytical expression for total reaction cross sections). This is also the case for the proposed analytical form since Eq. (2) defines a Gaussian function when ρ_p is small. Thus σ was determined by fitting the logarithm of the projected density under consideration versus b^2 using $b = R_0 + 2a$ and $b = R_0 + 4a$, where R_0 is the nuclear radius and a the diffuseness characterizing the Woods-Saxon density. As expected, σ varies approximately as $A^{1/3}$.

The values of $\rho_p(0)$ were taken directly from the numerical calculations. Approximately $\rho_p(0) \simeq 2\rho(0)r_0 A^{1/3}$ (Table I), where $\rho(0)$ is the central nuclear density and $r_0 A^{1/3} = R_0$.

The volume integral of the nuclear density is, of course, equal to the mass of the nucleus considered. Thus,

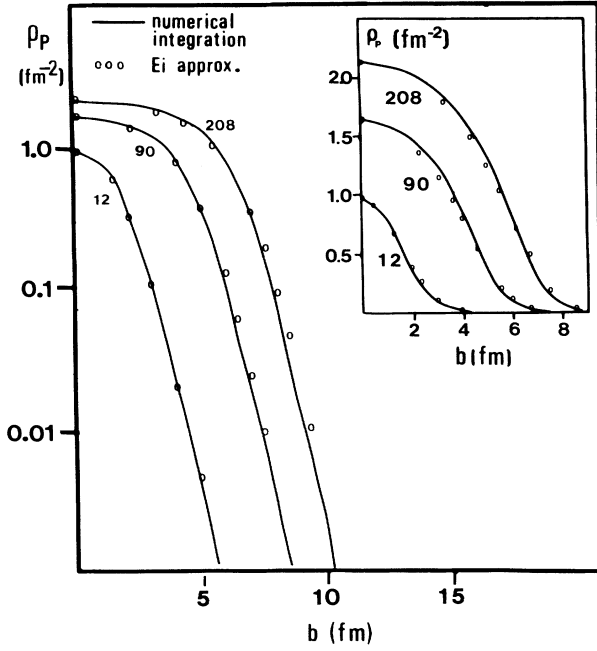


FIG. 1. Semilog plot of projected nuclear densities obtained by integrating Woods-Saxon forms along one Cartesian coordinate (solid lines) compared with results obtained using the exponential integral approximation (dots). The parameters for these calculations are given in Table I. A linear plot is also shown as an inset.

$$A = \int_0^{\infty} \rho_p(b) 2\pi b db. \quad (4)$$

However, from Eq. (2) we obtain

$$\begin{aligned} A &= \pi \int_0^{\infty} \rho_p(b) db^2 \\ &= 2\pi\sigma^2 \int_0^{\rho_p(0)} e^{k_p \rho_p} d\rho_p \\ &= \frac{2\pi\sigma^2}{k_p} (e^{k_p \rho_p(0)} - 1), \end{aligned} \quad (5)$$

which given σ and $\rho_p(0)$ may be solved (numerically) for k_p .

Parameters for atomic nuclei from ^{12}C to ^{208}Pb are given in Table I. This table is not intended to provide an accurate description for any particular nucleus, but rather to illustrate the variation of σ , $\rho_p(0)$, and k_p with mass number.

B. Calculation of cross section for a given number of nucleon-nucleon collisions

Using the analytical form [Eq. (2)], it is a simple matter to derive an expression for the cross section for exactly n nucleon-nucleon collisions. For example, if the probability distribution for n collisions takes on a Poisson distribution around the average value $T = \langle n \rangle$ (see Ref. 3), we have

$$P_n = T^n e^{-T} / n!, \quad (6)$$

$$\sigma_n = \int_0^{\infty} 2\pi b db T^n(b) e^{-T(b)} / n!, \quad (7)$$

with $T(b) = \bar{\sigma}_{\text{NN}} \rho_p$ and $k = k_p / \bar{\sigma}_{\text{NN}}$, we easily obtain

$$\begin{aligned} \sigma_n &= \{2\pi\sigma^2 / [n(1-k)^n]\} \\ &\times \left[1 - e^{-(1-k)T(0)} \right. \\ &\quad \left. \times \sum_{i=1}^n [(1-k)T(0)]^{n-i} / (n-i)! \right]. \end{aligned} \quad (8)$$

In Ref. 1 this quantity was supposed to follow a simple law $\sigma_n = cd^n$, where c and d are constants. Another quantity used in Ref. 1 was the average number of nucleon-nucleon collisions, the average being taken first over the straight line trajectory (z) and then over impact parameter (b). This quantity, of course, is zero if simply averaged over all impact parameters (to infinity). Thus the weighted average is defined through

$$\begin{aligned} \langle\langle n \rangle\rangle &= \langle T \rangle \\ &= \int_0^{\infty} T(1-e^{-T}) 2\pi b db / \int_0^{\infty} (1-e^{-T}) 2\pi b db, \end{aligned} \quad (9)$$

where the weighting is taken to be the reaction probability (the probability for >0 collisions). The denominator in Eq. (8) is thus simply the total reaction cross section

TABLE I. Geometrical properties of projected Woods-Saxon nuclear densities. $\rho(r) = 1 / \{1 + \exp[(r-R)/a]\}$. The diffuseness parameter (a) was set to 0.55 fm for all nuclei. The root mean square radii which were used to determine the radius parameters (R_0) are typical values from the compilation of RMSR for charge distributions (Ref. 15).

Mass (u)	Radius (fm)	Diffuseness (fm)	RMSR (fm)	σ (fm)	$\rho_p(0)$ (fm ⁻²)	k_p (fm ²)
12	1.743	0.55	2.450	1.443	0.967	0.09024
27	2.931	0.55	3.055	1.688	1.114	0.5176
40	3.588	0.55	3.430	1.790	1.208	0.7641
56	4.120	0.55	3.790	1.871	1.388	0.8748
90	4.825	0.55	4.260	1.952	1.634	0.9089
120	5.377	0.55	4.640	2.059	1.799	0.9016
152	6.018	0.55	5.090	2.155	1.851	0.9736
208	6.592	0.55	5.500	2.225	2.135	0.9212

σ_R , and using Eq. (2) the numerator is simply evaluated to yield

$$\langle\langle n \rangle\rangle = (2\pi\sigma^2/\sigma_R) [(e^{kT(0)} - 1)/k - (e^{(k-1)T(0)} - 1)/(k-1)], \quad (10)$$

where the first term evaluates to $\bar{\sigma}_{NN} \cdot A/\sigma_R$ [using Eq. (5)] and the second term, which was omitted in Ref. 1, represents a correction of roughly 5% for a Au target.

III. SIMPLIFIED PICTURE OF THE REACTION MECHANISM

Above ~ 200 MeV the free nucleon-nucleon total cross section^{7,9} is almost constant. We use a value of 40 mb for all energies in the range considered (0.3–20 GeV). We thus expect the number of primary nucleon-nucleon collisions to vary little with energy (assuming, even at the lowest energy, that $\bar{\sigma}_{NN}$ is not modified by the Pauli exclusion principle). The average kinetic energy E_0 (elastic) transmitted per collision to a struck nucleon in the target also becomes constant above ~ 1 GeV (see Ref. 8). Thus one might expect the physics of nucleon induced spallation to remain unchanged above this energy. This simple picture is somewhat modified due to the fact that above 1 GeV the free nucleon-nucleon total elastic cross section diminishes, giving way principally to the formation of delta resonances (inelastic nucleon-nucleon scattering) which decay mainly by pion emission. Following Abul Magd *et al.*,¹ we assume that the additional energy deposited in the target matter is proportional to the ratio of the inelastic cross section to the total nucleon-nucleon cross section,

$$E_0 = E_0(\text{elastic}) + 0.5\alpha(\sigma_{\text{inel}}/\sigma_{\text{total}})(m_\Delta - m_N), \quad (11)$$

where $m_\Delta - m_N$ is the delta-nucleon ground state mass difference (300 MeV) and the factor of $\frac{1}{2}$ comes from the fact that the inelastic excitation may be produced on the emerging high energy nucleon and thus not contribute to the deposition of excitation energy.

The parameter α ($\alpha < 1$) introduced in Eq. (11) is used to represent the rather complex situation resulting from the creation of delta resonances inside the target. This quantity was not used in Ref. 1. However, the decay of the delta resonance may lead to the ejection of a pion from the target and thus to the loss of the corresponding kinetic and rest energy.

In writing Eq. (11), of course we should be aware that the physical basis of the inelastic energy dissipation implied is unlikely to predominate above $E_p = 3$ GeV where delta production gives way to two- and three-pion production and reactions such as $p + p \rightarrow d + \pi^+$ become important (see Ref. 9). Indeed, we might expect that the complexity of the inelastic energy dissipation [which may be expressed in Eq. (11) as $\alpha(150 \text{ MeV})(\sigma_{\text{inel}}/\sigma_{\text{total}})$] would lead to an energy dependent value of α . However, since a detailed analysis of all mechanisms (and corresponding escape probabilities) is beyond the scope of the present work, we have preferred to retain a constant value for α in our calculations. As will be clear later (Sec. IV), the approximate constancy of the excitation

functions at high energies is a consequence of an increasingly wide “plateau” in the mass distributions, the height of which is only weakly influenced by changes in the excitation energy deposited in the target nucleus.

If we adopt this simple picture and, in addition, assume that the mass ejected from the target is proportional to the excitation energy, we can write

$$\langle dm_1 \rangle / dT = C(E_p), \quad (12)$$

where the slope C depends on the excitation energy and thus on the incident proton energy E_p , and m_1 is the mass lost from the target. Equation (12) may, in principle, also take into account promptly emitted nucleons (knock-out) since the number of such particles is also expected to be proportional to the number of primary nucleon-nucleon collisions. Of course, we expect that, because of the rather complex kinematical and geometrical situation which governs the emission or retention of struck nucleons in the target and, in addition, the importance of the sequential evaporation process which may involve emission of both nucleons and complex particles, the actual mass emitted when an incident proton traverses the target may be subject to considerable fluctuation around the mean. We (conveniently) assume a Poisson shape to describe this fluctuation $\sigma_{m_1}^2 = (CT)$. Thus,

$$P_{m_1}(T) = (CT)^{m_1} e^{-CT} / m_1!. \quad (13)$$

The advantage of this procedure is that we may immediately [as in Eqs. (6)–(8)] write the expression for the cross section σ_{m_1} ($m_1 = A - A_F$, where A_F is the observed fragment mass) as

$$\sigma_{m_1} = \{2\pi\sigma^2/[m_1(1-k/C)^{m_1}]\} \times \left[1 - e^{-(C-k)T(0)} \times \sum_{i=1}^{m_1} [(C-k)T(0)]^{m_1-i} / (m_1-i)! \right], \quad (14)$$

in which C is the only unknown parameter. Since the average number of collisions is approximately four [using Eq. (10)], we have chosen to ignore the prompt knock-out contribution in describing the energy variation of this parameter (as in Ref. 1), which will thus be specified using Eq. (11).

IV. CALCULATION AND RESULTS

Calculations were made of excitation functions for specific residual nuclei for protons incident on a Au target in the energy range from 0.3 to 20 GeV and compared with the data reported in the work of Kauffman and Steinberg.¹⁰ The constant C of Eq. (13) was fixed by comparing measured and calculated mass distributions at 3 GeV to a value of 8.8 u per nucleon-nucleon collision. We then used the estimation of the mean excitation energy per unit mass loss (ϵ), which was calculated by the authors of Ref. 1 using the evaporation model of Friedman and Lynch¹² to calculate the parameter α of

Eq. (11). With $\epsilon = 13.2$ MeV, we obtain $\alpha = 0.5$. The resulting variation of the energy deposited per nucleon-nucleon collision is shown in Fig. 2(a). At each energy the quantity C [in Eq. (14)] was fixed by scaling the value fitted to the data at 3 GeV by the ratio of excitation energies deposited in the target per nucleon-nucleon collision.

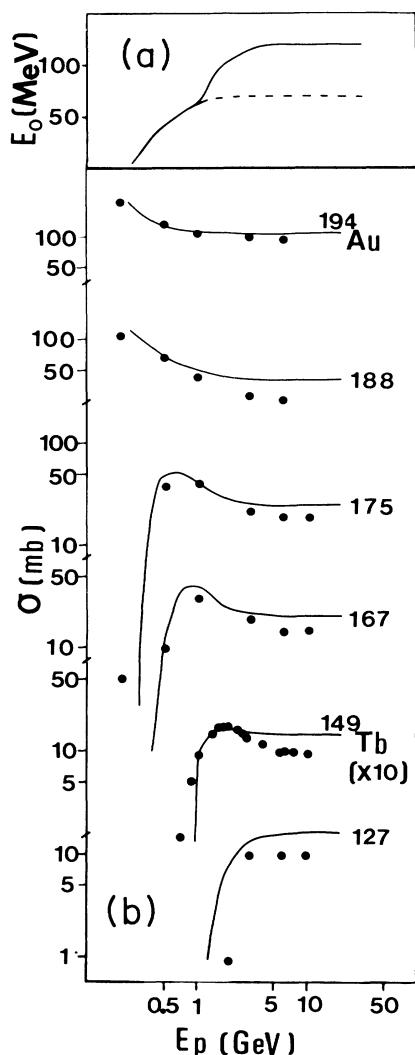


FIG. 2. (a) Variation with incident proton energy of the total energy deposited per nucleon-nucleon collision in target matter (solid line). The energy deposited due to elastic scattering alone is indicated by the dotted line [see Eq. (11)]. (b) Excitation functions for various spallation products compared with the calculations [Eq. (14)]. The data are from Refs. 10 and 11 (^{159}Tb). The ^{194}Au yield, which is known to represent only a fraction of the mass 194 cross section, has been multiplied by 3.33. The ^{159}Tb data (Ref. 11) are for the alpha decay branch, which is thought to represent $\sim 10\%$ of the cross section (see Ref. 10). The measured cross section has thus been multiplied by 10 and the calculation normalized arbitrarily to the data. The experimental and theoretical normalization for all other cases is absolute.

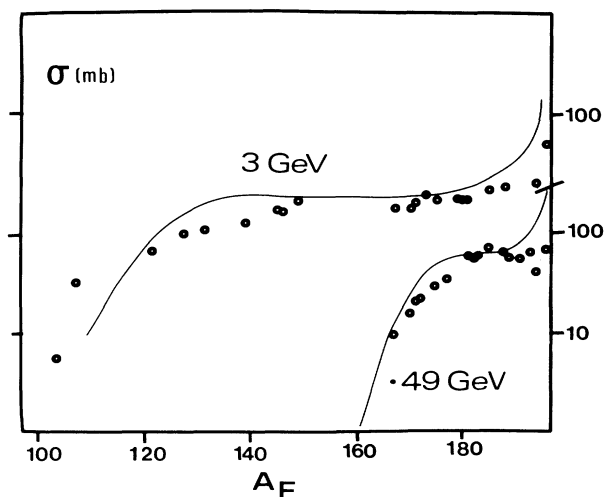


FIG. 3. Calculated and measured (Ref. 10) mass distributions following proton spallation reactions on a Au target at 0.49 and 3 GeV incident proton energies. The 3 GeV data were used to fix the parameter C of Eq. (12), which was scaled for other energies by the ratio of the excitation energy deposited in the target to the same quantity at 3 GeV [see text and Fig. 2(a)]. The shape of the calculated (solid lines) and observed (dots) distributions is discussed in the text. The measured cross sections for isotopes near the target are lower limits due to the strong probability in this region for (undetected) stable nuclide production. Otherwise, errors in the data are typically of the order of 10%. Normalization, for both experiment and calculations, is absolute.

Excitation functions calculated using Eq. (14) for mass losses between 3 and 70 u are presented with the data in Fig. 2(b). As can be seen from the figure, the overall agreement is quite satisfactory. The measured cross sections are however up to a factor of 2 smaller than the predictions at the highest energies.

In addition, we have calculated the residual mass distributions at 0.49 and 3 GeV. The agreement with the data (see Fig. 3) is once again very satisfactory. Both the data and the calculation show cross sections which fall steeply as we descend below the target mass followed by a plateau which extends to mass losses of $\sim C\bar{\sigma}_{\text{NN}\rho_p}(0)$ corresponding to a zero impact parameter trajectory after which the cross section falls sharply. These three regions can be readily distinguished in Eq. (14). The “plateau” is produced by the geometrical factor $1/(1-k/C)^{m_1}$, whereas the cutoff [term in large parentheses in Eq. (14)] is caused by the fact that the average number of nucleon-nucleon collisions, and thus the average mass loss maximizes at zero impact parameter. The initial steep falloff of the cross section for masses close to that of the target is approximately given by $2\pi\sigma^2/m_1$ and is thus energy independent.

V. SUMMARY AND CONCLUSIONS

In this work we have presented a simple model for proton induced spallation reactions in which the main

emphasis has been placed on a rather accurate parametrization of projected nuclear densities, which permits a simple analytical form to be derived for the spallation product cross sections. Mass distributions and excitation functions have been calculated for protons incident on a Au target using a much simplified description of the physics of spallation reactions inspired by previous work.^{1,2} The one parameter appearing in this simple model is the average mass evacuated from the target per primary nucleon-nucleon collision. Its energy variation was assumed to follow the energy deposition of the incident proton in the target.

Very good agreement was obtained with excitation functions measured by Kauffmann and Steinberg¹⁰ despite the simplicity of the model and the neglect of the fission channel. It is probable that this neglect mainly affects cross sections for rather central collisions, i.e., leads to an overestimate of the cross sections near the cutoff point and, of course, to an absence of predicted

cross section significantly below the cutoff.

We should perhaps mention that Eqs. (2) and (3) may prove quite useful in other problems where projected nuclear densities are used. Typical examples are the microscopic ablation abrasion model of Hüfner, Shafer, and Schurman,¹³ and the linear cascade model of Knoll and Randrup.¹⁴

In Ref. 1 the authors derived an expression for the spallation cross section that was exponential in form. Indeed, the geometry of projected nuclear densities was approximated in such a way as to produce this dependence. The approximation used is quite good for light nuclei, but works less well for heavy targets. For light nuclei the "plateau" region is very narrow and the cross section shows an almost monotonic falloff. In this respect we feel that the present work presents an appreciable improvement over the treatment presented by Abul-Magd, Friedman, and Hüfner.

*Permanent address: Faculty of Science, University Mohamed V, Rabat, Morocco.

¹A. Y. Abul-Magd, W. A. Friedman, and J. Hüfner, *Phys. Rev. C* **34**, 113 (1986).

²X. Campi and J. Hüfner, *Phys. Rev. C* **24**, 2199 (1981).

³A. J. Cole, *Z. Phys. A* **322**, 313 (1985).

⁴R. J. Glauber, *Lectures on Theoretical Physics* (Interscience, New York, 1959), Vol. 1.

⁵A. J. Cole, *Phys. Rev. C* **35**, 117 (1987).

⁶P. J. Karol, *Phys. Rev. C* **11**, 1203 (1975).

⁷L. Ray, *Phys. Rev. C* **20**, 1878 (1979).

⁸G. J. Igo, *Rev. Mod. Phys.* **50**, 523 (1978).

⁹O. Benary, L. R. Price, and G. Alexander, University of

California-Lawrence Radiation Laboratory Report 20000 NN, 1970.

¹⁰S. B. Kauffman and E. P. Steinberg, *Phys. Rev. C* **22**, 167 (1980).

¹¹E. M. Franz and G. Friedlander, *Nucl. Phys.* **76**, 123 (1966).

¹²W. A. Friedman and W. G. Lynch, *Phys. Rev. C* **28**, 16 (1983).

¹³J. Hüfner, K. Schafer, and B. Schurmann, *Phys. Rev. C* **12**, 1888 (1975).

¹⁴J. Knoll and J. Randrup, *Nucl. Phys.* **A324**, 445 (1979).

¹⁵C. W. de Jager, H. de Vries, and C. de Vries, *At. Data Nuclear Data Tables* **14**, 479 (1974).